Title	Neoproterozoic Mafic-Ultramafic Intrusions from the Fanjingshan Region, South China: Implications for Subduction-Related Magmatism in the Jiangnan Fold Belt
Author(s)	Wang, W; Zhao, JH; Zhou, MF; Yang, SH; Chen, FK
Citation	The Journal of Geology, 2014, v. 122 n. 4, p. 455-473
Issued Date	2014
URL	http://hdl.handle.net/10722/216904
Rights	The Journal of Geology. Copyright © University of Chicago Press.

Neoproterozoic Mafic-Ultramafic Intrusions from the Fanjingshan Region, South China: Implications for Subduction-Related Magmatism in the Jiangnan Fold Belt

Wei Wang,[1,2] *Jun-Hong Zhao,*[1,*] *Mei-Fu Zhou,*[2] *Sheng-Hong Yang,*[3] *and Fu-Kun Chen*[4]

1. State Key Laboratory of Geological Processes and Mineral Resources, China University of Geosciences, Wuhan 430074, People's Republic of China; 2. Department of Earth Sciences, University of Hong Kong, Hong Kong SAR, People's Republic of China; 3. Department of Geosciences, University of Oulu, 90014 Oulu, Finland; 4. School of Earth and Space Sciences, University of Science and Technology of China, Hefei 230026, People's Republic of China

ABSTRACT

The Jiangnan Fold Belt was formed through the collision of the Yangtze and Cathaysia Blocks during the Neoproterozoic. The ca. 820 Ma mafic-ultramafic rocks from the Fanjingshan region in the western Jiangnan Fold Belt, South China, are composed mainly of olivine pyroxenite, clinopyroxenite, and gabbros with minor wehrlite. Olivine pyroxenites have low and constant K_2O (<1 wt%) and Na_2O (<0.17 wt%) and a narrow range of $\varepsilon_{Nd(t)}$ (−3.2 to −1.6) and $^{207}Pb/^{204}Pb$ (15.65–15.89), suggesting insignificant crustal contamination. They have high Os (0.182–1.70 ppb), low Re/Os (0.29–2.24) and γ_{Os} (−1.9 to +20.3), indicating their origination from a heterogeneous mantle source. By contrast, two gabbros have γ_{Os} values ranging from 179 to 243, which may have resulted from later addition of Re and minor crustal contamination. Olivine pyroxenites and calculated parental magmas show similar primitive mantle–normalized trace element patterns with variable depletion of high field strength elements (e.g., Nb, Ta Zr, Hf, and Ti) and enrichment of large-ion lithophiles (e.g., Th, U, Rb, and Pb). Their Sr-Nd-Pb isotopic compositions are also similar to those of enriched mantle II–type mantle. These features are consistent with magma derived from a mantle wedge that was previously metasomatized by slab-derived fluids and melts. The mafic-ultramafic rocks from Fanjingshan have bulk rock and mineral compositions similar to those of Alaskan-type intrusions, suggesting that they were formed in a subduction-related environment just before amalgamation of the Yangtze and Cathaysia Blocks.

Online enhancements: supplementary tables.

Introduction

The Jiangnan Fold Belt, formed by the amalgamation of the Yangtze and Cathaysia Blocks during the Neoproterozoic, is important for the understanding of Precambrian crustal accretion and tectonic evolution of South China and its link with the supercontinent Rodinia (Zhou et al. 2002, 2008; Li et al. 2008*c*, 2009; Zhao and Cawood 2012; Zheng et al. 2013). Igneous rocks are widely distributed in the Jiangnan Fold Belt and are characterized by granitoids, volcanic rocks, and minor mafic-ultramafic intrusions with ages ranging from 830 to 750 Ma (Li et al. 1999; Ge et al. 2001; Wang et al. 2008; Zhou et al. 2009; Zhang et al. 2012*a*; Zhao and Zhou 2013). Mafic-ultramafic rocks in the Jiangnan Fold Belt are crucial in constraining the formation and evolution of the Jiangnan Fold Belt as well as its correlation with the assembly and breakup of Rodinia, but their origin has been a matter of debate for decades (Zhou et al. 2008, 2009; Xue et al. 2012). Their tectonic affinity is explained by either mantle plume, arc subduction, or plate rift (Li et al. 2003*a*, 2008*a*, 2008*b*; Wang et al. 2006*b*; Wu et al. 2006; Zheng et al. 2008; Zhao and Zhou 2013), but the nature of their mantle source region and petrogenesis are still poorly constrained.

Osmium is highly compatible and rhenium is moderately incompatible during partial melting of

Manuscript received August 13, 2013; accepted March 13, 2014; electronically published June 19, 2014.

* Author for correspondence; e-mail: jhzhao@cug.edu.cn.

[The Journal of Geology, 2014, volume 122, p. 455–473] 0022-1376/2014/12204-0007$15.00. DOI: 10.1086/676596

mantle. Substantial fractionation occurs between Re and Os during crustal accretion and hence discriminative Os isotopic compositions between mantle and crust are generated through time (Shirey and Walker 1998). Therefore, the Re-Os system is a long-lived radiogenic isotope system sensitive to the nature of mantle source and crustal assimilation of mantle-derived magmas (Shirey and Walker 1998).

Mafic-ultramafic rocks may contain clinopyroxene that can be used to investigate the evolution and petrogenetic processes of mantle-derived magmas (Johnson et al. 1990; Rampone et al. 1993; Ross and Elthon 1993; Bizimis et al. 2000; Rivalenti et al. 1996). Large-ion lithophile elements (LILEs) and high field-strength elements (HFSEs) are incompatible in clinopyroxene but less so than these elements are in olivine and spinel (Stosch and Seck 1980; Green 1994). Thus, clinopyroxene is the main carrier of these trace elements and can be used to examine the nature of mantle-derived magmas (Johnson et al. 1990; Rampone et al. 1993; Ross and Elthon 1993; Rivalenti et al. 1996; Bizimis et al. 2000). Chemical compositions of primary clinopyroxene can provide reliable information about the processes of mantle melting, metasomatism, and subsolidus reequilibration (Johnson et al. 1990; Suhr et al. 1998).

We chose mafic-ultramafic rocks from Fanjingshan, the western Jiangnan Fold Belt for detailed study. New Sr-Nd-Pb-Os isotopic data are integrated with trace element compositions of clinopyroxene in order to investigate the nature of mantle source of the rocks and further to constrain the tectonic affinity of these rocks.

Geological Background

The Jiangnan Fold Belt records a series of complex tectonic events from ca. 970 to ca.750 Ma (Li et al. 2003*a*, 2003*b*; Wang et al. 2006*b*, 2013; Zheng et al. 2008, 2013; Zhao et al. 2011; Wang and Zhou 2012; Zhang et al. 2012*b*; Zhao and Cawood 2012; Zhao and Zhou 2013). Tectonically, the Fanjingshan region in northeastern Guizhou Province is the western segment of the Jiangnan Fold Belt (fig. 1*a*). The Neoproterozoic Fanjingshan Group crops out over an area of ~270 km^2, with thicknesses ranging from 7,500 to 11,620 m (fig. 1*b*; Wang and Li 2003; Wang et al. 2010*a*; GRGST 1974).

The Fanjingshan Group is divided into upper and lower parts based on lithologic variations. The lower part consists of sandstone, siltstone, tuff, sericite phyllite, and slate with abundant pillow lavas, representing a shallow marine volcanic–sedimentary system (GRGST 1974; BGMRGZ 1987). Individual pillows of pillow lava are 25–60 cm long and 12–35 cm wide and exhibit vesicular and amygdaloidal textures. These rocks are highly altered and many are mapped as spilites based on their very high Na_2O contents (GRGST 1974; BGMRGZ 1987). The upper part is characterized by terrigenous turbidite with flysch structures and consists of sandstone, siltstone, and phyllite (GRGST 1974; BGMRGZ 1987). The Fanjingshan Group and its equivalents, the Lengjiaxi, Sibao, Shuangqiaoshan, and Xikou Groups, throughout the Jiangnan Fold Belt were recently dated at 830–815 Ma (Gao et al. 2008, 2010; Wang et al. 2010*b*, 2012*a*, 2012*b*, 2013; Zhao et al. 2011). Overlying the Fanjingshan Group is the late Neoproterozoic Xiajiang Group and Nanhua-Sinian system, which are covered by strongly deformed Paleozoic to Lower Mesozoic, shallow marine deposits (Yan et al. 2003; Chu et al. 2012*a*, 2012*b*).

Field Relations and Petrography

Mafic-ultramafic bodies from the Fanjingshan region are distributed in NE-trending belt and occur mainly along stratification planes of the Fanjingshan Group (fig. 1*c*). They are approximately 10 m thick and 10~20 km long. In spite of strong deformation, intrusive contacts of some intrusions with their country rocks were preserved (BGMRGZ 1987; Zhang et al. 2008). These rocks consist of wehrlite, olivine pyroxenite, clinopyroxenite, and gabbro (Zhang et al. 2008). Most of the rocks are hydrothermally altered to different degrees, and their primary minerals are partially to completely replaced by serpentine, tremolite, chlorite, epidote, and sericite (GRGST 1974; BGMRGZ 1987).

Wehrlite consists of clinopyroxene and olivine, which is largely replaced by serpentine. Accessory minerals include chromite, magnetite, and sulphide. Associated olivine pyroxenites are composed of up to 75% clinopyroxene with less abundant olivine (5%~25%) and biotite (1%) associated with minor chromite and sulfide. Most of these rocks have poikilitic textures with rounded olivine grains enclosed in clinopyroxene (fig. 2). Primary clinopyroxene grains in olivine pyroxenites are euhedral to subhedral, 1–2 mm across (fig. 2*a*–2*c*), whereas secondary clinopyroxenes are smaller (0.4–0.8 mm) and show subhedral to anhedral morphologies (fig. 2*d*, 2*e*). Magnetite occurs mainly as inclusions in clinopyroxene. Small (0.08–0.1 mm), euhedral magnetite grains are sporadically distributed in interstices between clinopyroxene and olivine. Other minerals include plagioclase, chromite, ilmenite, and pentlandite (fig. 2). Gabbro has poikilitic and

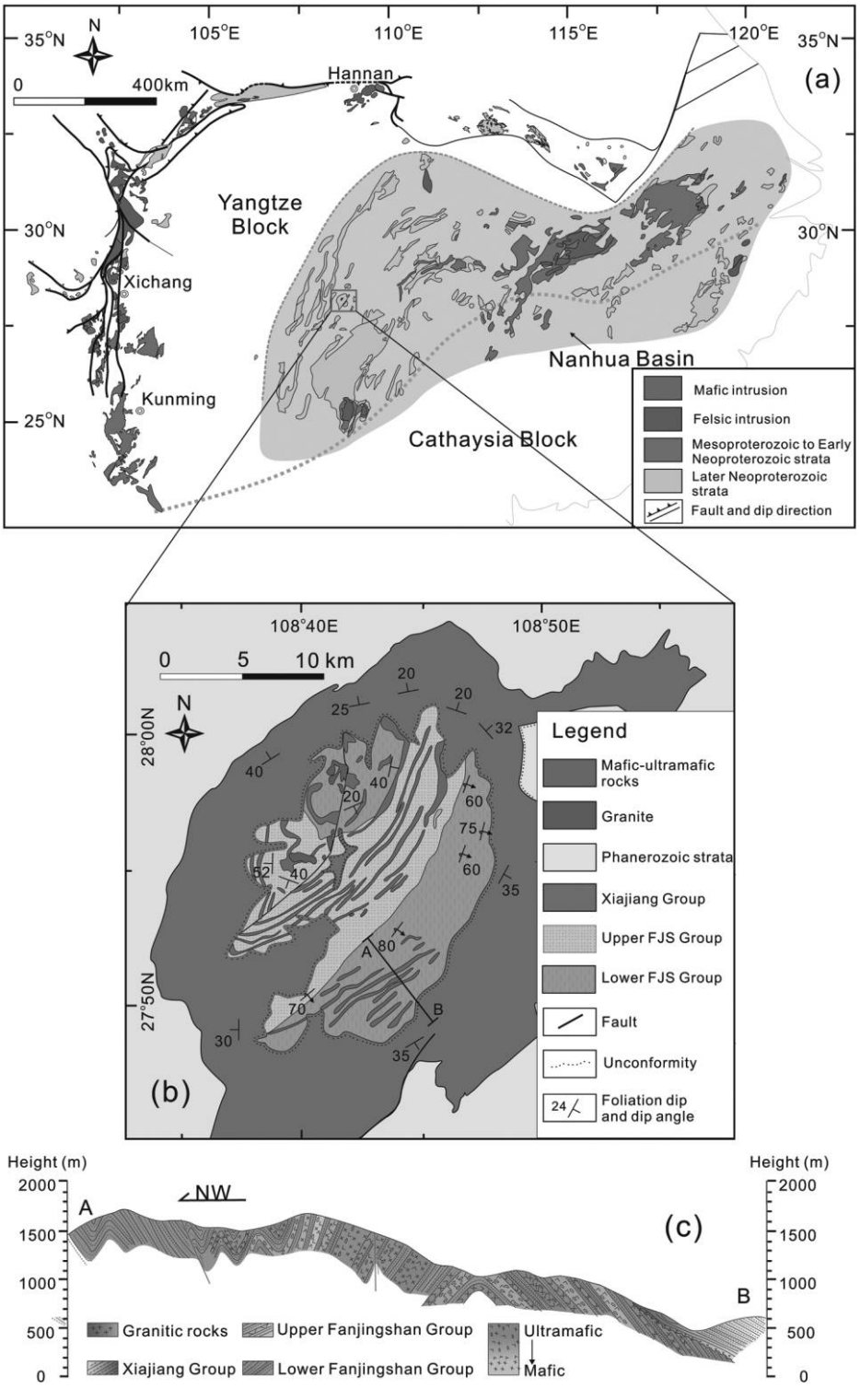

Figure 1. Sketch geological map of the studied area. *a*, Framework of South China containing the Yangtze Block in the northwest and the Cathaysia Block in the southeast (modified after Zhao et al. 2011). Primary Precambrian geological units including sedimentary sequences, mafic to felsic igneous plutons, and major faults are highlighted in the Yangtze Block. *b*, Geological map of the Fanjingshan area (FJS) showing the distribution of mafic-ultramafic rocks (modified after GRGST 1974). *c*, General cross section involving major units of the Fanjingshan area (modified after GRGST 1974). A color version of this figure is available online.

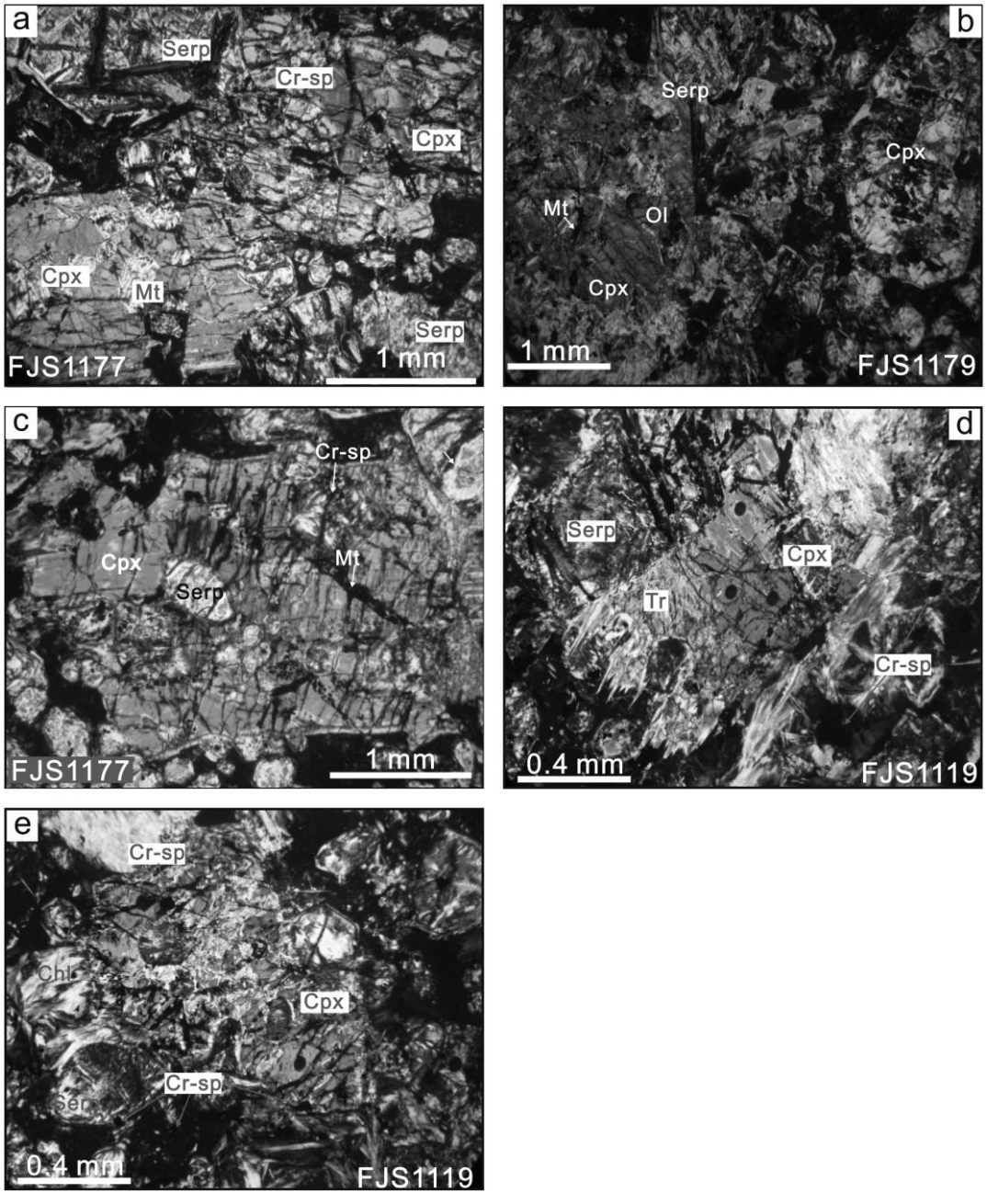

Figure 2. Photomicrographs of rocks from Fanjingshan. Serp = serpentine; Cr-sp = Cr-spinel; Cpx = clinopyroxene; Mt = magnetite; Ol = olivine; Tr = tremolite; and Chl = chlorite. A color version of this figure is available online.

ophitic textures and consists chiefly of plagioclase and pyroxene with minor quartz and titanite.

Analytical Methods

Laser Ablation (LA)-ICP-MS U-Pb Dating of Zircon. U-Pb isotope analysis of zircon was carried out by LA-ICP-MS at the State Key Laboratory of Ore Deposit Geochemistry, Institute of Geochemistry, Chinese Academy of Sciences (CAS), Guiyang. A combination of a GeoLasPro laser ablation system and an Agilent 7700x ICP-MS was used for the analyses. The 193-nm ArF excimer laser, homogenized by a set of beam delivery systems, was focused on the zircon surface with a fluence of 10 J/cm^2. The ablation protocol employed a spot diameter of 32 μm at a 5-Hz repetition rate for 45 s. Helium was employed as a carrier gas to allow efficient trans-

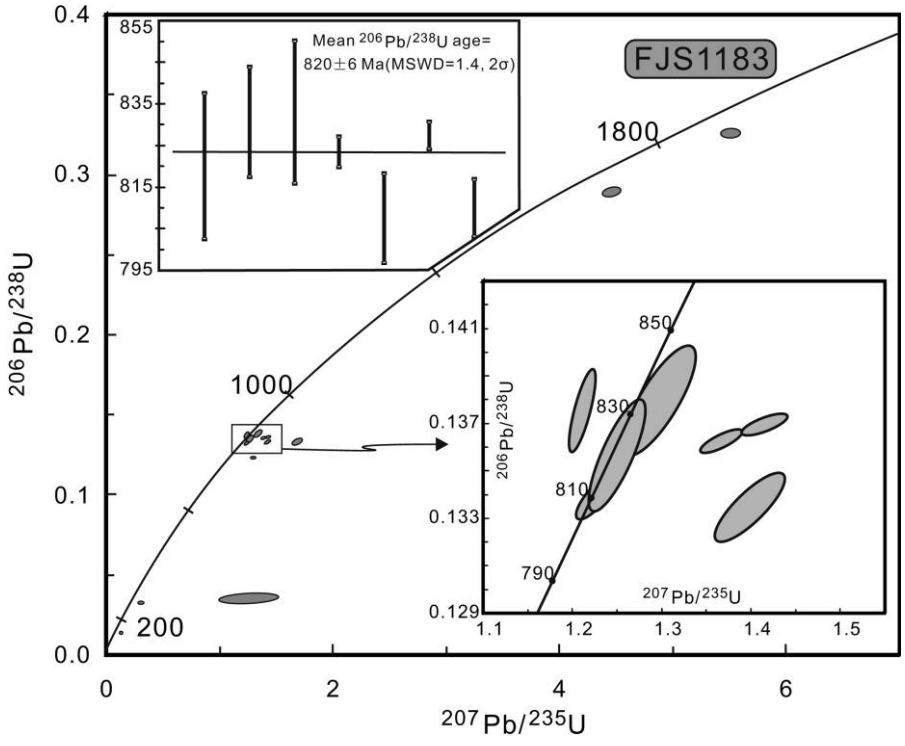

Figure 3. Concordia plots of laser ablation ICP-MS U-Pb dating of zircons separated from sample FJS1183.

port of aerosol to the ICP-MS. Raw data reduction was performed offline by ICPMSDataCal (Liu et al. 2010). Data were processed using the ISOPLOT program (Ludwig 2003).

Bulk Rock Major and Trace Elements. Major element abundances were obtained using X-ray fluorescence (XRF) on fused glass beads at the University of Hong Kong. Trace elements were analyzed on a Quadrupole ICP-MS at the State Key Laboratory of Ore Deposit Geochemistry, Institute of Geochemistry, CAS, Guiyang.

Closed beakers in high-pressure bombs with 1 mL HF and 1 mL HNO_3 were used to ensure complete digestion. This analytical procedure is particularly suitable for analyzing Zr and Hf because zircon is completely dissolved with a recovery of nearly 100%. Pure elemental standards for external calibration, and OU-1 and AMH-1 were used as reference materials. Accuracies of the XRF analyses are estimated to be 2% for most major elements and 1% for SiO_2. Details are given in (Qi et al. 2000). ICP-MS analyses for trace elements have accuracies better than 5% for all investigated trace elements.

Bulk-Rock Isotopes Analyses. Rb-Sr and Sm-Nd isotopic analyses were carried out using a Finnigan MAT-262 mass spectrometer, located at the CAS Key Laboratory of Crust-Mantle Material and Environment, University of Science and Technology of China. Our analytical procedure is similar to that of Chen et al. (2002, 2007). Sample powders were spiked with mixed isotope tracers, dissolved in Teflon capsules with $HF+HNO_3$, and separated by conventional cation-exchange techniques. Strontium and rare earth elements (REEs) were separated and purified on quartz columns by conventional ion-exchange chromatography with a 5-mL resin bed of AG 50W-X12 (200–400 mesh) after sample decomposition. Nd and Sm were further separated from other REEs on quartz columns using 1.7-mL Teflon powder coated with HDEHP, di(2-ethylhexyl)orthophosphoric acid, as cation exchange medium. Pb was separated using anion exchange techniques with diluted HBr as an eluant. Measured $^{87}Sr/^{88}Sr$ and $^{143}Nd/^{144}Nd$ ratios were corrected for mass fractionation relative to $^{86}Sr/^{88}Sr = 0.1194$ and $^{146}Nd/^{144}Nd = 0.7219$, respectively. Total procedural blanks were <200 pg for Sr, <50 pg for Nd, and <200 pg for Pb. Analytical precisions of isotope compositions are given as 2σ standard errors, and errors of initial isotopic ratios are quoted at the 2σ level.

For Re-Os isotope analyses, 2–3 g sample powders were accurately weighted and dissolved using an improved Carius tube technique described by Qi et al. 2010, in the State Key Lab of Ore Deposit Geochemistry, Institute of Geochemistry (SKLODG),

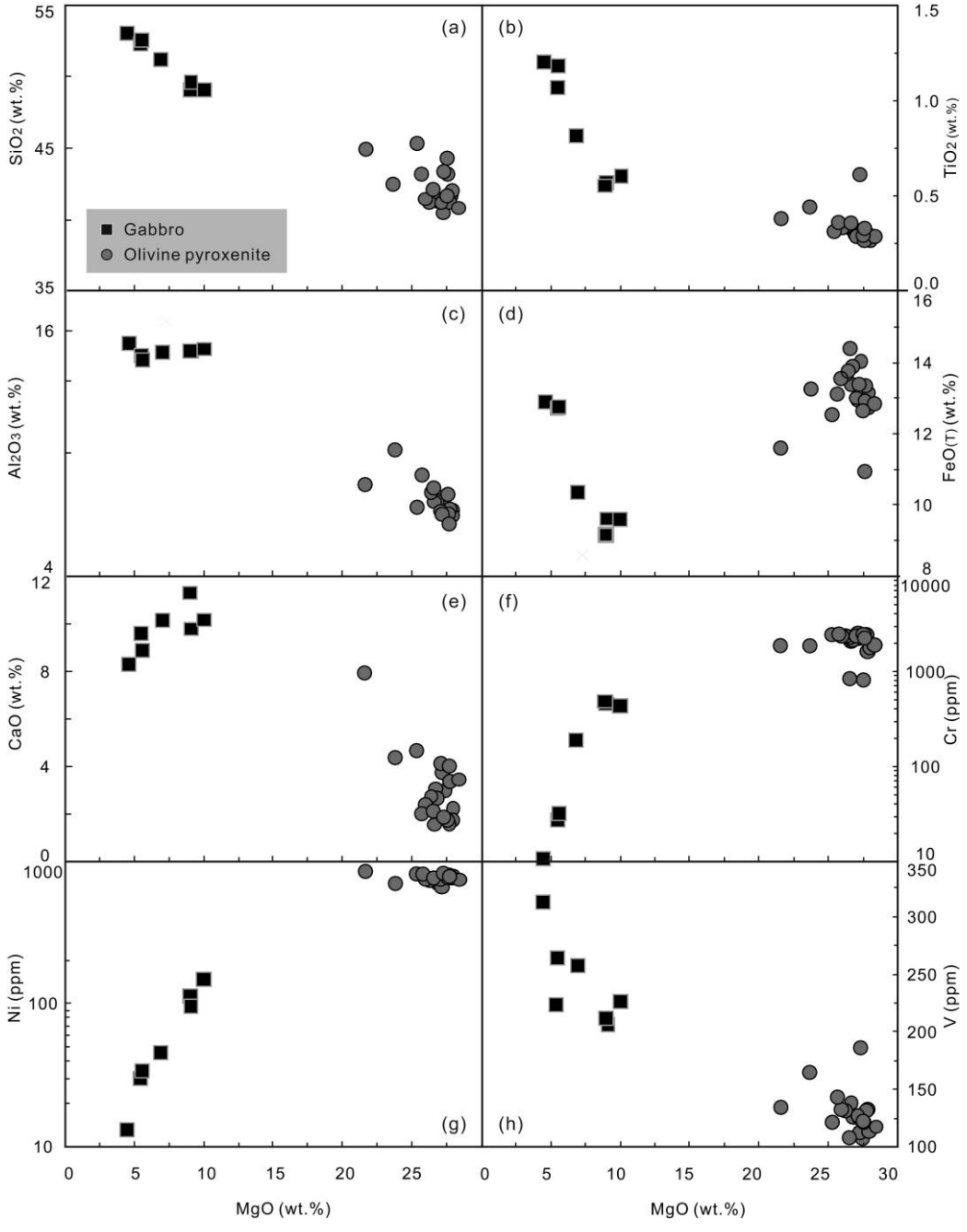

Figure 4. Major oxides and trace elements versus MgO variation diagrams for bulk-rock geochemistry of mafic-ultramafic rocks from Fanjingshan.

CAS, Guiyang. Immersed in an ice-water bath, the Carius tube was added in approximate amounts of ^{185}Re and ^{190}Os spikes with 10 mL purified concentrated HNO_3 and 2 mL purified concentrated HCl. The Carius tubes were kept at ~240°C in an oven for 48–72 h. After that, Os was distilled as OsO_4 from the matrix using in situ distillation equipment. Re was separated from the matrix and purified by anion exchange resin (Biorad AG 1 × 8, 200–400 mesh). Os isotopic ratios were measured on a Thermo-Finnigan Triton mass spectrometer with negative ion detection mode and equipped with an oxygen gas leak valve and an ion-counting multiplier in Guangzhou Institute of Geochemis-

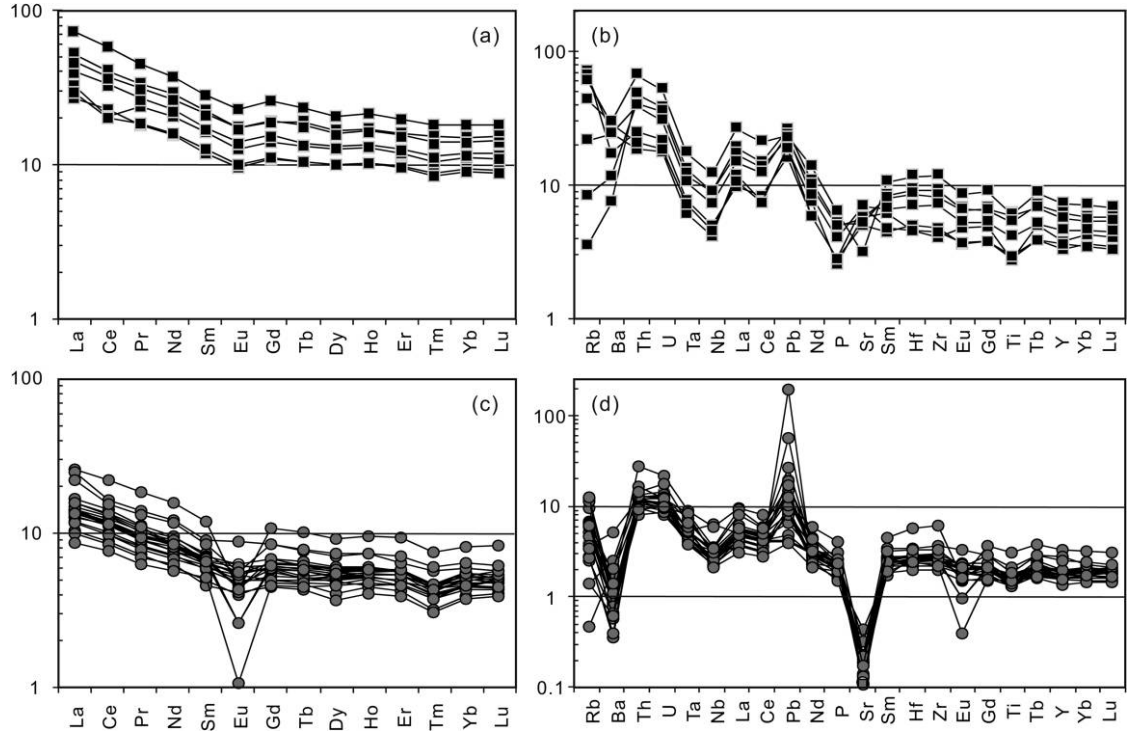

Figure 5. Chondrite-normalized rare earth element patterns and primitive mantle-normalized trace element spider diagrams for bulk-rock compositions of mafic-ultramafic rocks from Fanjingshan. Normalized values are from Sun and McDonough (1989). Symbols are the same as in figure 4.

try, CAS. Re isotopes were measured using a PE ELAN DRC-e ICP-MS in SKLODG. Total procedural blanks of Re and Os were 6.4 and 2.0 pg.

Electron Microprobe and In Situ Trace Element Analysis. Major element compositions of clinopyroxene were obtained with a JEOL JXA8100 electron microprobe at the Guangzhou Institute of Geochemistry, China. The standards used were olivine for Mg and Si, garnet for Al, diopside for Ca, omphacite for Na, ilmenite for Ti, chromite for Cr, fayalite for Fe, and niccolite for Ni. Peak and background counting times were set at 20 s and 10 s, respectively. Samples were analyzed with a focused beam in spot mode at an accelerating voltage of 15 kV and a beam current of 20 nA.

Trace element concentrations of clinopyroxene were determined by a Resonetic M50 193-nm excimer laser coupled to a Thermo PQ Excell LA-ICP-MS at the Department of Earth Sciences, University of Hong Kong. Each analysis was performed by ablating spots with 40 μm diameter at 6 Hz with energy of ~100 mJ per pulse. Helium was employed as the carrier gas. USGS standards BHVO-2G, BCR-2G, and BIR-1G were used as external standards, and GSE-1G was analyzed as an unknown sample for quality control. The sum of all element concentrations expressed as oxides (according to their oxidation states present in the silicates) are considered to be 100% m/m for a given anhydrous silicate mineral (Liu et al. 2008; Chen et al. 2011). NIST610 was used as an internal standard. The offline data processing was performed by ICPMSDataCal (Liu et al. 2010).

Analytical Results

Zircon U-Pb Dating. Euhedral zircon grains from a gabbroic sample (FJS1183) have uniform to oscillatory-zoned internal structures and high Th/U ratios (0.35–3.19), typical features of magmatic zircon. Among 14 grains analyzed (table S1; tables S1–S5 available online), 9 analyzed grains have concordant $^{206}Pb/^{238}U$ ages of 808 Ma to 833 Ma, with a weighted mean age of 820 ± 8 Ma (MSWD = 1.4), which is considered as the emplacement age of the gabbro (table S1; fig. 3).

Whole-Rock Chemical Compositions. Representative whole-rock major and trace element compositions of olivine pyroxenites and gabbros are given in table S2. Olivine pyroxenites have narrow ranges

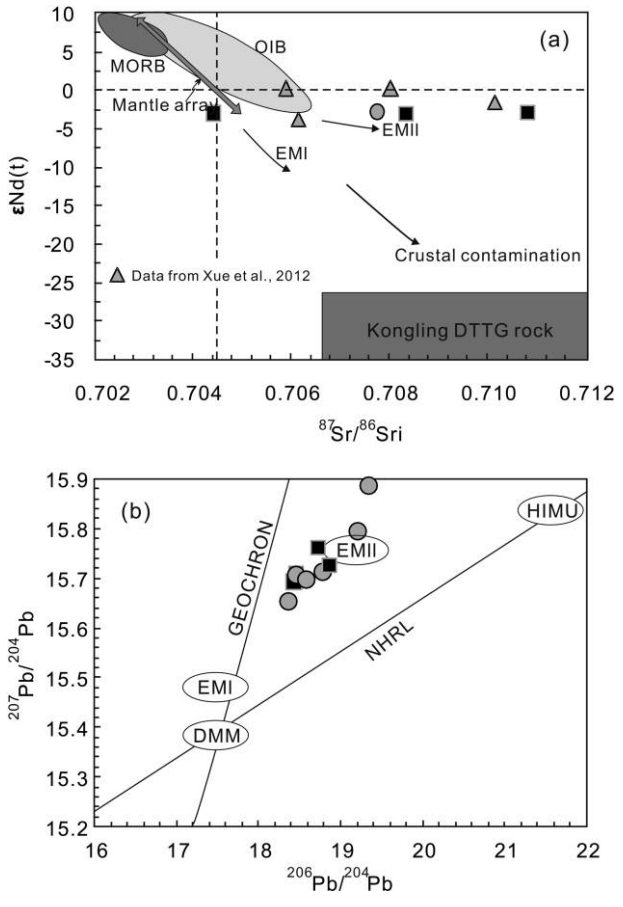

Figure 6. *a*, Plots of initial $^{87}Sr/^{88}Sr$ versus $\varepsilon_{Nd(t)}$ values for mafic-ultramafic rocks from Fanjingshan. Midocean ridge basalt (MORB), mantle array, and enriched mantle (EM)I and EMII trends are after Zindler and Hart (1986). Ocean island basalt (OIB) data are from Wilson (1989). Data for Kongling dioritic-tonalitic-trondhjemitic-granodioritic (DTTG) rocks are from Gao et al. (1999) and Zhang (2008). *b*, Plots of $^{206}Pb/^{204}Pb$ versus $^{207}Pb/^{204}Pb$ for mafic-ultramafic rocks from Fanjingshan. The fields of high-μ mantle (HIMU), depleted MORB mantle (DMM), EMl, and EMll are from Weaver (1991) and Zindler and Hart (1986). Northern Hemisphere Reference Line (NHRL) is from Hart (1984). Symbols are the same as in figure 4.

of SiO_2 (40.5–45.3 wt%), TiO_2 (0.27–0.62 wt%), Al_2O_3 (5.3–8.2 wt%), MgO (21.7–28.4 wt%), and $FeO^{(T)}$ (10.9–14.4 wt%). Similarly, gabbros have generally uniform SiO_2 (49.1–53.0 wt%), TiO_2 (0.56–1.21 wt%), and Al_2O_3 (13.6–14.9 wt%) but variable MgO (4.5–10.0 wt%) and $FeO^{(T)}$ (9.2–12.9 wt%). In all the rocks, SiO_2, TiO_2, and Al_2O_3 correlated negatively, and $FeO^{(T)}$ correlated positively with MgO (fig. 4).

Olivine pyroxenites exhibit chondrite-normalized REE patterns with slight enrichment of LREE (La/Yb_N = 1.76–3.96), flat HREE (Gd/Yb_N = 0.99–1.39) and mostly variable negative Eu anomalies (Eu/Eu^* = 0.22–1.03). Gabbros have relatively uniform chondrite-normalized REE patterns with slight enrichment of LREE (La/Yb_N = 2.69–3.71), flat HREE (Gd/Yb_N = 1.14–1.39) and slightly negative Eu anomalies (Eu/Eu^* = 0.83–0.86). In the primitive mantle–normalized trace element spider diagram, the olivine pyroxenites are characterized by strong depletion of Ba and Sr, slight depletion of Nb and Ta, moderate enrichment of Th and U, and strong enrichment of Pb (fig. 5). In contrast, gabbros are significantly depleted in Nb, Ta, P, and Ti but enriched in Th, U, La, and Pb.

Sr, Nd, and Pb Isotopes. Sr-Nd-Pb isotopic compositions are presented in table S3. Gabbros have relatively constant $\varepsilon_{Nd(t)}$ (−3.2 to −2.1), and variable $^{87}Rb/^{86}Sr$ (0.250 to 1.023) and $^{87}Sr/^{86}Sr$ ratios (0.711287 to 0.723042). By contrast, olivine pyroxenites have slightly more depleted Nd isotopes with $\varepsilon_{Nd(t)}$ ranging from −3.0 to −1.7. One olivine pyroxenite has $^{87}Rb/^{86}Sr$ of 1.025 and $^{87}Sr/^{86}Sr$ of 0.719827.

Two olivine pyroxenites (FJS1189 and FJS1190) have high $^{206}Pb/^{204}Pb$ (19.196–19.331), $^{207}Pb/^{204}Pb$ (15.793–15.890) and $^{208}Pb/^{204}Pb$ (40.332–40.386); the other samples have similarly low $^{206}Pb/^{204}Pb$ (18.364–18.865), $^{207}Pb/^{204}Pb$ (15.653–15.761), and $^{208}Pb/^{204}Pb$ (38.737–39.501). All samples plot above the Northern Hemisphere Reference Line (NHRL) and nearby to the enriched mantle (EM)II end-member (fig. 6*b*).

Re-Os Isotopes. Re-Os isotopic data are presented in table S4 and plotted on the isochron diagram in figure 7. Errors of $^{187}Os/^{188}Os$ ratios are estimated on the basis of replicate analyses of laboratory reference samples and includes uncertainties in mass-spectrometry, both in run precision and in fractionation correction by normalization.

Whole-rock Re concentrations for all samples from Fanjingshan are variable, from 0.111 to 0.975 ppb. Olivine pyroxenites have Re (0.297–0.605 ppb) higher than the gabbros (0.111–0.233 ppb), but one gabbro has the highest Re of 0.975 ppb. Olivine pyroxenites have common Os concentrations (0.182–1.701 ppb) higher than those of the gabbros (0.006–0.083 ppb). Olivine pyroxenites have variable $^{187}Os/^{188}Os_i$ (calculated back to 820 Ma) ratios between 0.1197 and 0.1468, whereas two gabbros (FJS1168 and FJS1183) have highly radiogenic $^{187}Os/^{188}Os_i$ ratios of 0.3402 and 0.4191, while the other two gabbros (FJS1101 and FJS1115) have unreasonably low $^{187}Os/^{188}Os_i$ ratios of 0.0691 and –1.9896.

Compositions of Clinopyroxene. Clinopyroxenes have diopsidic to augitic compositions (fig. 8). They

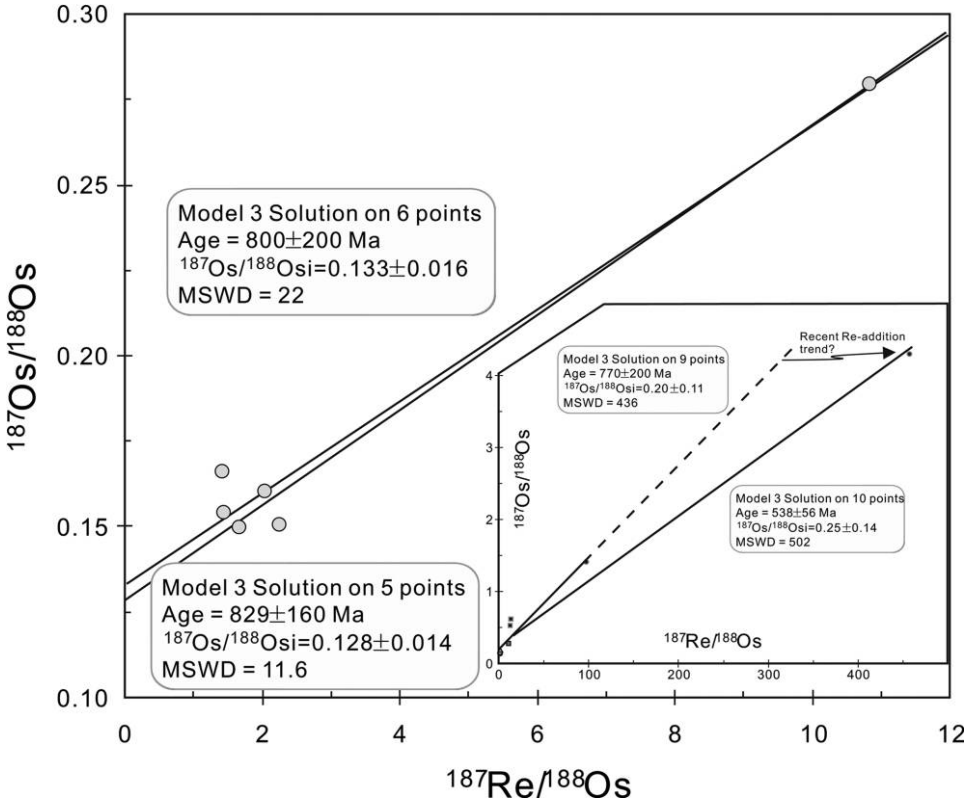

Figure 7. Re-Os isochron of mafic-ultramafic rocks from Fanjingshan. The errors of $^{187}Re/^{188}Os$ and $^{187}Os/^{188}Os$ are estimated to be 3% and 2%, respectively. A color version of this figure is available online.

have low Al_2O_3 (0.40–2.98 wt%) and Na_2O (0.15–0.83%) and high $FeO^{(T)}$ (4.72–9.42 wt%), Cr_2O_3 (0–0.95 wt%), and TiO_2 (0.04–0.80 wt%) (table S5). There are positive correlations between of Mg# versus TiO_2 and SiO_2 versus Al_2O_3. Clinopyroxenes of olivine pyroxenites have higher Mg# values (81.4–86.0) than those in gabbros (75.9–84.0).

Clinopyroxenes have generally flat chondrite-normalized REE patterns with distinct depletion of LREE (La/Yb_N = 0.32–0.65) and slightly positive Eu anomalies (Eu/Eu^* = 0.77–1.31; fig. 9*a*, table S5). They show primitive normalized-trace element patterns with negative Sr, Zr, and Ti anomalies (fig. 9*b*).

Discussion

Alteration and Metamorphism. Mafic-ultramafic rocks from the Fanjingshan region may have undergone low-temperature hydrothermal alteration, greenschist facies metamorphism, and strong tectonic deformation along with their country rocks (GRGST 1974). During these processes, their chemical compositions may have been partially modified. Nevertheless, immobile elements, such as HFSEs and REEs, are resistant to these secondary processes and can be used to constrain the petrogenesis of altered mafic-ultramafic rocks (Wang et al. 2006*a*; Zhao and Zhou 2007). Although K and Rb are suspected to be mobile during alteration (Zhao and Zhou 2007), K_2O/Rb ratios for most olivine pyroxenites (95–251) and all gabbros (213–448) are relatively constant, suggesting these elements were not affected by alteration. In addition, the mafic and ultramafic rocks have similar REE patterns with constant La/Yb_N (1.76–3.96) and Gd/Yb_N (0.99–1.39) values, indicating immobility of REE during alteration.

Hydrothermal alteration of Re has been reported for a number of layered mafic-ultramafic intrusions (Hart and Kinloch 1989; Lambert et al. 1994; Marcantonio et al. 1994). Slight variation of Re/Os ratios would significantly change initial Os isotopic compositions corrected back to the time of emplacement (ca. 820 Ma). One olivine pyroxenite with high $^{187}Re/^{188}Os$ ratio of 10.8 has $^{187}Os/^{188}Os_i$ similar to other olivine pyroxenites which have relatively low $^{187}Re/^{188}Os$ ratios (1.4–2.3), indicating Re-Os isotopic system remained close after magma emplacement. By contrast, two gabbro samples have

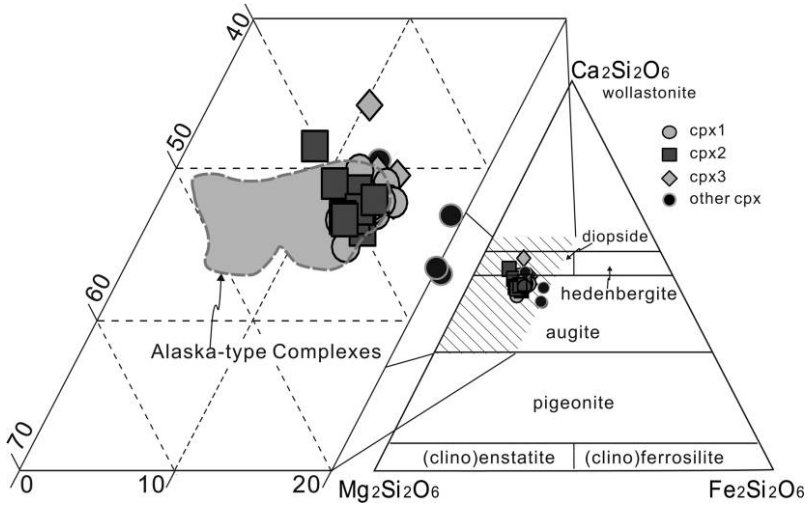

Figure 8. Clinopyroxene compositions of olivine pyroxenite from Fanjingshan. The gray field with dashed line boundary corresponds to the compositions of clinopyroxene in Alaskan-type complexes (Himmelberg and Loney 1995; Irvine 1974; Helmy and El Mahallawi 2003).

low Os concentrations and strong negative γ_{Os} values (–43 and –1731), suggesting disturbance of the Re-Os isotope system in these samples.

Magmatic Differentiation and Crustal Contamination. Magmatic differentiation is considered as a major process controlling the compositional variations of mafic-ultramafic rocks from the Fanjingshan region (fig. 4). The negative correlation between MgO and Cu/Ni ratios suggests that olivine and orthopyroxene played an important role in the magma evolution. Olivine pyroxenites have a negative correlation between SiO_2 and MgO and a positive correlation between Ni and MgO. They also have CaO and CaO/Al_2O_3 ratios negatively correlated with MgO, indicating olivine accumulation (fig. 4). However, gabbros that experienced olivine fractionation display a positive correlation between CaO and MgO, reflecting fractionation of clinopyroxene (fig. 4). Negative correlations of TiO_2 and V with MgO imply that magnetite did not crystallize during the magma evolution. The strongly negative Sr and Eu anomalies of olivine pyroxenites may reflect plagioclase fractionation.

Although they show positive Th and U anomalies and negative Nb and Ta anomalies in the primitive mantle–normalized diagram (fig. 5*b*), olivine pyroxenites have low and constant K_2O and Na_2O and lack positive Zr-Hf anomalies, inconsistent with significant crustal contamination. Depletion of Zr and Hf in clinopyroxene from the olivine pyroxenites (fig. 9*b*, 9*d*) further demonstrate that their parental magmas were not significantly modified by crustal contamination. Olivine pyroxenites have slightly variable $\varepsilon_{Nd(t)}$ and $^{207}Pb/^{204}Pb$ ratios that are irrelevant to MgO content (fig. 10), indicating that the discrepant isotopic compositions were more likely inherited from heterogeneous parental magmas. Gabbros have $\varepsilon_{Nd(t)}$ values and $^{207}Pb/^{204}Pb$ ratios similar to those of olivine pyroxenites, both defining fractional crystallization trend and indicating limited crustal contamination.

Osmium isotopic compositions of olivine pyroxenites also argue for insignificant crustal contamination. Because crustal materials usually have higher Re/Os and $^{187}Os/^{188}Os$ ratios but lower Os concentrations relative to mantle-derived magmas (Shirey and Walker 1998), $^{187}Os/^{188}Os_i$ of the magma experienced crustal contamination is supposed to be negatively correlated with Os concentration but positively correlated with $^{187}Re/^{188}Os$, which is opposite to the relationship exhibited by olivine pyroxenites (fig. 11). Therefore, the heterogeneity of initial Os isotopic compositions (0.1197 and 0.1468) of olivine pyroxenites more likely indicate replenishing magma in an open-system magma chamber.

On the other hand, two gabbro samples have high γ_{Os} values (179 to 243) that are negatively correlated with Mg#, implying significant crustal assimilation during the magma emplacement. This phenomenon could be explained by the compatible features of Os during magma fractional crystallization, which dramatically decrease Os concentration in the evolved magma. Thus, low Os contents in the evolved magma makes Os isotope system much more sensitive to crustal contamination relative to

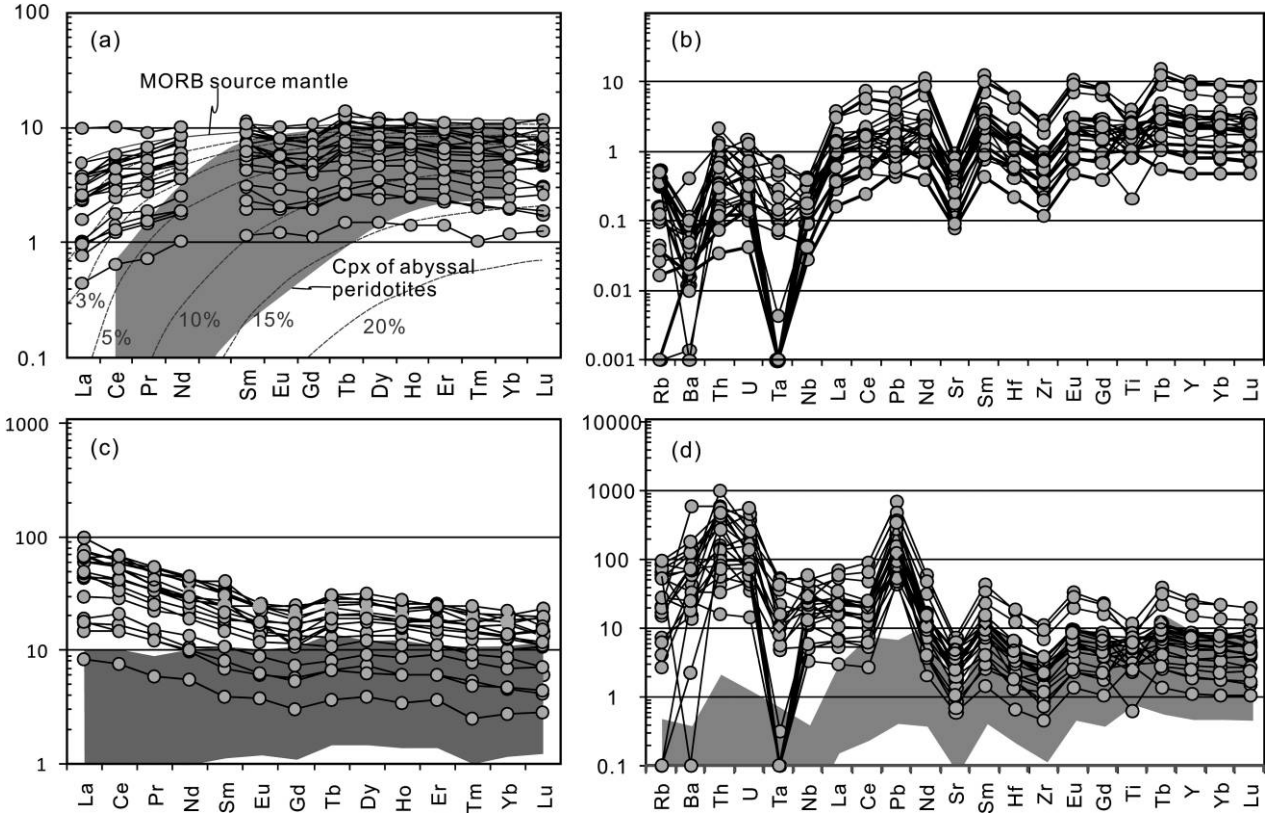

Figure 9. Chondrite-normalized rare earth element (REE) patterns (*a*) and primitive mantle-normalized trace element spider diagrams (*b*) for the clinopyroxene from olivine pyroxenites. Chondrite-normalized REE patterns (*c*) and primitive mantle-normalized trace element spider diagrams (*d*) for geochemical compositions of the parental magma in equilibrium with clinopyroxene from the olivine pyroxenites. Clinopyroxene/liquid partition coefficient used for calculation are from Bédard (2001). Normalized values are from Sun and McDonough (1989). Shaded areas in *c* and *d* are the compositions of clinopyroxene. Also shown in the REE-normalized diagram (*a*) is fractional melting modeling of residual clinopyroxene after extraction of melt from spinel stability field mantle. MORB = midocean ridge basalt. A color version of this figure is available online.

Nd and Pb ones. On the other hand, the decoupling of Os from Sr-Nd isotopic systems was also observed in the evolution of some basaltic magmas, evidencing interaction with sulfide-rich crustal materials and leading the assimilation of Os than Sr-Nd was assimilated into the silicate magma due to the chalcophile nature of Os (cf. Yang et al. 2012). Therefore, selective contamination of Os isotopes could be the possible mechanism to explain the highly radiogenic Os isotopic composition of gabbros in Fanjingshan.

Subduction-Related Enrichment of Mantle Source. Mafic and ultramafic rocks from the Fanjingshan region have low $\varepsilon_{Nd(t)}$ values, and high and variable $^{87}Sr/^{88}Sr$ ratios, as well as high Pb isotopic ratios, which are similar to those of EMII-type mantle source (fig. 6*a*, 6*b*). Olivine pyroxenites have subchondritic to slightly radiogenic γ_{Os} values (-1.9 to $+20.3$), indicating a heterogeneous mantle source. The least radiogenic sample has $^{187}Os/^{188}Os_i$ of 0.1197, similar to that of subcontinental lithospheric mantle ($^{187}Os/^{188}Os_{820Ma} = 0.1155–0.1193$; Zheng et al. 2009), indicating involvement of lithospheric mantle in their parental magma. On the other hand, the radiogenic samples with high γ_{Os} values could be derived from an enriched mantle source because crustal contamination has been excluded (see above).

Addition of slab-derived radiogenic Os can substantially change the Os isotopic signatures of suprasubduction lithospheric mantle (Brandon et al. 1996, 1999; Widom et al. 2003; Saha et al. 2005). This mechanism is very appealing to explain the highly radiogenic Os nature as well as the wide range of Os isotopic compositions of the mantle source of mafic-ultramafic rocks from the Fanjingshan region. The positive correlation between $^{187}Os/^{188}Os_i$ ratios and La/Sm and Rb/Y indicate ad-

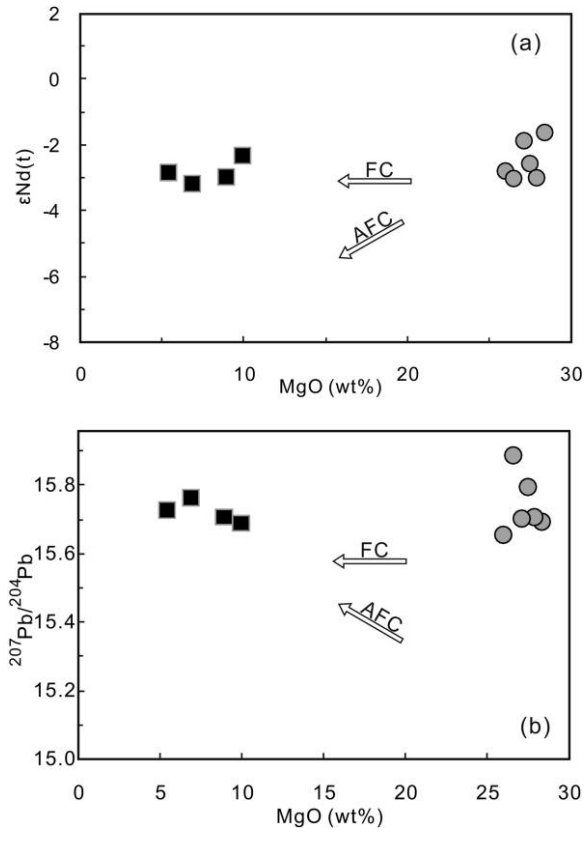

Figure 10. Plots of $\varepsilon_{Nd(t)}$ and $^{207}Pb/^{204}Pb$ versus MgO (wt%) for mafic and ultramafic rocks from Fanjingshan. Mentioned in the text are FC (fractional crystallization) and AFC (assimilation fractional crystallization). Symbols are the same as in figure 4.

dition of radiogenic Os into the suprasubduction mantle through circulation of hydrous fluids. These ratios are thought to be sensitive to the slab-derived fluids modification (Maury et al. 1992). The continuous influx of radiogenic Os into the mantle wedge would also generate highly radiogenic γ_{Os} values of +20 even though the slab-fluids have Os concentration much lower than that of the mantle wedge (cf. Widom et al. 2003).

Mafic-ultramafic rocks from the Fanjingshan region have high Th and U concentrations, implying high-temperature fluid fluxing in the mantle source (Hermann et al. 2006). Their elevated Rb/Y and Th/Zr ratios relative to constant Nb/Y and Nb/Zr ratios (fig. 12*a*, 12*b*) suggest addition of Rb and Th to the mantle wedge by hydrous fluids (Maury et al. 1992). Slab-derived fluids have low and constant K/Rb ratios, whereas slab-derived melts have high K/Rb ratios but low K and Rb abundances (Kogiso et al. 1997; Zhao and Zhou 2007). The rocks from Fanjingshan have relatively low K/Rb ratios (fig. 12*c*), further confirming metasomatism of their mantle source region by hydrous fluids. Hydrous fluids are able to transport Nd more effectively than Hf, so the decoupling of Hf-Nd isotopic signatures of gabbro from Fanjingshan (Zhou et al. 2009) is also indicative of fluid metasomatism.

Compositions of clinopyroxene can be used to estimate elemental concentrations of their parental magmas. The calculated compositions of the parental magma are rich in light REEs (LREEs) relative to heavy REEs (HREEs) with slightly negative Eu anomalies (fig. 9*c*, 9*d*). The melt has arc-like primitive mantle-normalized trace elemental patterns with enrichment of LILEs (e.g. Rb, Ba, and Th) and strong depletion of HFSEs (e.g., Nb, Ta, Zr, and Hf; fig. 9*d*). However, Nb and Ta abundances are much lower than the experimentally estimated solubility of these elements in clinopyroxene in equilibrium with a slab-derived aqueous fluid (Baier et al. 2008), probably due to occurrence of Ti-bearing minerals during dehydration of downgoing slab (Xiong et al.

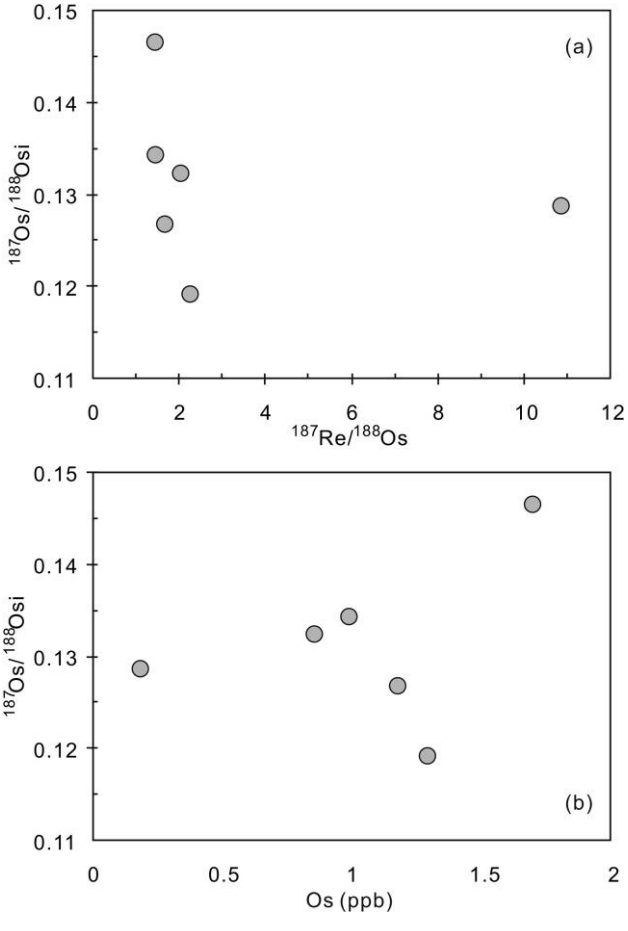

Figure 11. Plots of $^{187}Os/^{188}Os_i$ versus common Os and $^{187}Re/^{188}Os$ of mafic-ultramafic rocks from Fanjingshan.

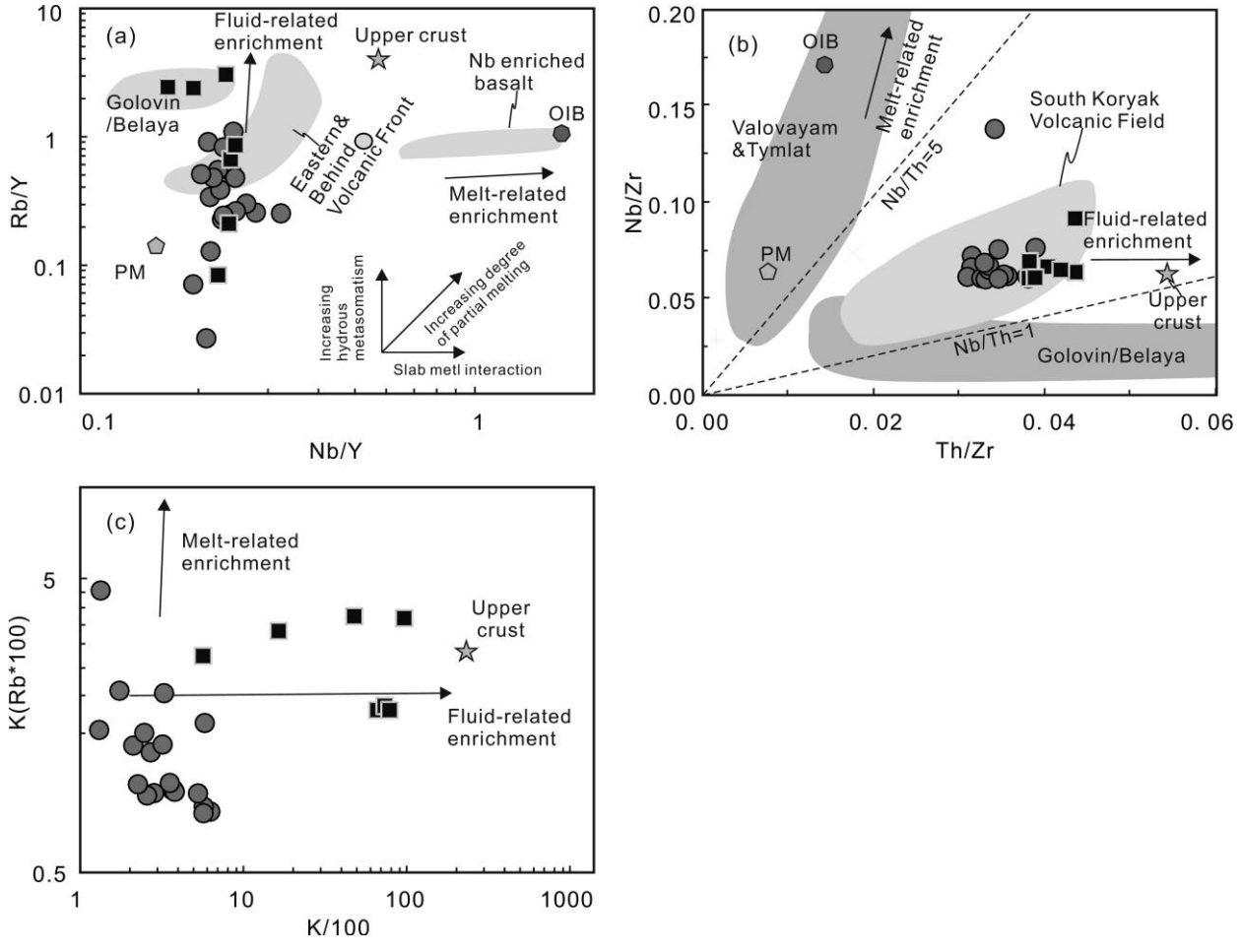

Figure 12. Binary diagrams illustrating the different metasomatic trend of rocks imposed by slab-released fluids or slab-derived melts. The values of primitive mantle (PM) and ocean island basalt (OIB) are from Sun and McDonough (1989). The values of upper crust are from Rudnick and Gao (2003). Fields of Valovayam and Tymlat, South Koryak Volcanic Field, Golovin/Belaya, Eastern and Behind Volcanic Front, and Nb-enriched basalt are from Kepezhinskas et al. (1997) for comparison. Symbols are the same as in figure 4.

2005). Ta is generally depleted relative to Nb in clinopyroxene and therefore in the parental magma in equilibrium with clinopyroxene (fig. 9*d*), perhaps reflecting fluid-related metasomatism because Ta has lower solubility in fluids than Nb and a clinopyroxene-fluid partition coefficient lower than that of Nb (Baier et al. 2008). The low concentrations of Zr, Hf, and Ti indicate no addition of these elements by slab-melt metasomatism (Grégoire et al. 2001; McInnes et al. 2001).

Partial Melting of the Mantle Wedge. Mafic-ultramafic rocks from Fanjingshan display moderate REE fractionation (La/Ybn = 1.76–3.96) and flat HREE patterns (Gd/Ybn = 0.99–1.39), indicating that they were derived from garnet-free mantle sources (Green 1994), probably from a spinel lherzolite mantle source.

Clinopyroxene that crystallized in the magma chamber is assumed to have the same trace element compositions as those of the residual clinopyroxene from the mantle source, if near-fractional melts separated in equilibrium with the mantle source and suffered no chemical modification en route to the crust and if the clinopyroxene/melt partition coefficients are constant (Suhr et al. 1998). The immobile trace elements (such as HREEs, Ti, and Zr) in clinopyroxene therefore can be used to estimate the degree of partial melting that the mantle source suffered (Jean et al. 2010). Calculations reveal that mainly 5%–10% fractional melting of spinel lherzolite could produce HREE compositions similar to those of clinopyroxene from olivine pyroxenites (fig. 9*c*). The LREE enrichment of these clinopyroxene probably reflects modification by slab-

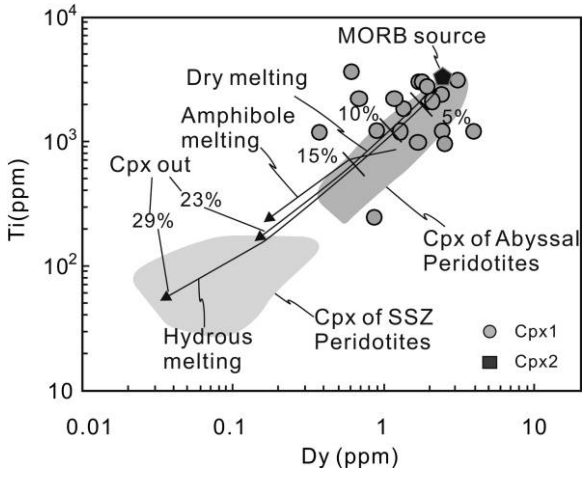

Figure 13. Geochemical modeling of the partial melting process in the mantle source. Ti versus Dy concentrations in clinopyroxene after Bizimis et al. (2000). Dry melting: residual clinopyroxene compositions during dry melting; hydrous melting: suggested refertilization-hydrous melting model; amphibole melting: melting of a midocean ridge basalt (MORB) source in the presence of amphibole (Bizimis et al. 2000). Fields for clinopyroxene in the suprasubduction zone (SSZ; Batanova and Sobolev 2000; Bizimis et al. 2000) and in abyssal peridotites (Johnson et al. 1990) are cited for comparison.

derived fluids, similar to refertilized clinopyroxene in residual peridotites from Happo-O'ne, central Japan (Khedr et al. 2010). A reverse modeling using Ti and Dy also indicates that 5%–10% melting of spinel lherzolite can produce residual clinopyroxene with HREE signatures similar to those of clinopyroxene of olivine pyroxenites from Fanjingshan (fig. 13). Nevertheless, it should be noted that the composition of accumulated clinopyroxene may be changed during its reequilibration of crystal with a residual liquid and in that case its trace element content (e.g., REE) tends to be slightly higher than the original composition (Godel et al. 2011). Consequently, the calculated degree of partial melting could be underestimated or a minimum value.

Implications for the Tectonic Setting. The negative correlations of Mg# versus TiO_2 and Al_2O_3 of clinopyroxene (fig. 14*a*, 14*b*) are indicative of differentiation of hydrous subduction-related magmas (Conrad and Kay 1984; DeBari and Coleman 1989; Loucks 1990). Clinopyroxene from studied mafic-ultramafic rocks have low Al_2O_3 and high SiO_2 (fig. 14*c*), similar to typical Alaskan-type intrusions, such as the Tulameen Complex in British Colombia (Rublee 1994), also suggesting crystallization from hydrous magmas. It is also characterized by low TiO_2 contents and low Al in tetrahedral sites (fig. 14*d*), typical of clinopyroxene from arc cumulative rocks (Loucks 1990). The calculated parental magma of olivine pyroxenites resembles those with an arc-affinity (fig. 9), also suggestive of an arc-related environment for the mafic-ultramafic rocks from the Fanjingshan region. The mantle beneath a subduction zone is suggested to have higher oxygen fugacity (Carmichael 1991). Vanadium (V) is very sensitive to the oxygen fugacity of mantle source, and a trend of increasing incompatibility from V^{3+} to V^{4+} to V^{5+} for all mineral phases has been identified (Mallmann and O'Neill 2009). Therefore, mantle melting under higher oxygen fugacity tend to generate magmas with high V content. Clinopyroxene of olivine pyroxenites from Fanjingshan have comparable or higher V content than some clinopyroxenes with similar Mg# from the Gaositai intrusion from the northern North China Craton, which is considered to have derived from a subduction zone (Chen et al. 2009). Accordingly, the high V values of clinopyroxene from olivine pyroxenites from Fanjingshan are indicative of a high oxygen fugacity environment, such as a subduction setting, for the generation of parental magmas.

The volcano-sedimentary sequence of the Fanjingshan Group can also provide constraints on the tectonic affinity of the associated mafic-ultramafic rocks (Zhou et al. 2009; Wang et al. 2010*a*; Zhao et al. 2011). Sedimentation of the Fanjingshan Group, and its equivalents, including the Lengjiaxi, Sibao, and Shuangqiaoshan Groups in the Jiangnan Fold Belt, was likely continuous until 830–820 Ma. These rocks are interpreted as flysch to molasse deposits accumulated in back-arc or retro-arc foreland basins (Wang and Zhou 2013; Wang et al. 2013). The ca. 820-Ma mafic-ultramafic rocks from Fanjingshan are nearly coeval with cessation of sedimentation of the Fanjingshan Group (Zhou et al. 2009; Wang et al. 2010*a*; Zhao et al. 2011), suggesting that the intrusions were related to subduction-related magmatism before amalgamation of the accreted terrane with the Yangtze Block. This conclusion is consistent with those derived from the studies of 825–829 Ma high-Mg boninitic rocks in the central part (Zhang et al. 2012*b*; Zhao and Zhou 2013) and of the ca. 824-Ma ophiolitic complex in the northeastern part of the Jiangnan Fold Belt (Zhang et al. 2012*a*). Taken together, the age and nature of these various units are suggestive of an arc development, back-arc extension and subsequent terrane accretion or continental collision. Such a scenario would be broadly analogous to the emplacement

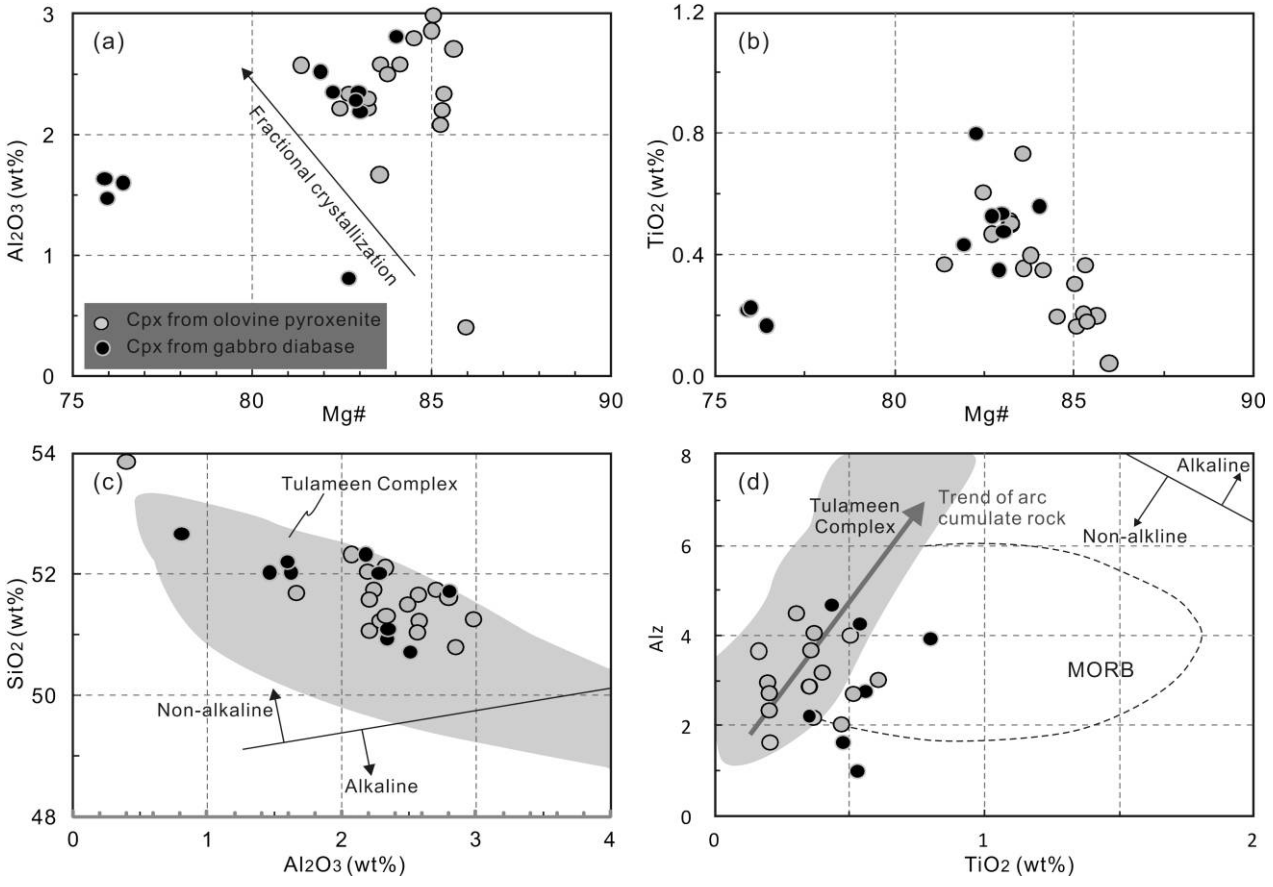

Figure 14. Clinopyroxene composition of rocks from Fanjingshan. The discrimination diagrams are after Le Bas (1962) and Pettigrew and Hattori (2006), where Alz refers to the percentage of Al in the tetrahedral sites (Alz = $100^{*IV}Al/2$). The trend for arc cumulate rocks in *d* represents pyroxene formed in hydrous arc magmas (Loucks 1990). Data from a typical Alaska-type complex, the Tulameen Complex (Rublee 1994), are exhibited for comparison. The term "nonalkaline" includes rocks with tholeiitic, high-alumina, and calc-alkaline affinity (Le Bas 1962).

of Alaskan-type intrusions, which commonly intrude during terrane accretion following subduction of oceanic crust and probably corresponds to the final phase of accretion of arc terrenes to continents (Saleeby 1992; Foley et al. 1997; Ayarza et al. 2000; Grenne et al. 2003).

Conclusions

The mafic-ultramafic rocks from the Fanjingshan region, west Jiangnan Fold belt, South China, formed at ca. 820 Ma. Parental magmas were likely produced by 5%–10% fractional melting of a suprasubduction lithospheric mantle corresponding to spinel peridotites equilibrated with the spinel stability field. This mantle source has been previously enriched by slab-released fluids above a subducting zone. This metasomatized mantle was heterogeneous in terms of subchondritic to slightly radiogenic Os isotopic compositions and supplied multiple replenishing magmas to an open-system magma chamber to form the Fanjingshan intrusions. Crustal contamination was insignificant during the ascent and emplacement of the basaltic parental magmas, whereas crustal material played an important role as evidenced by the Os isotopic compositions during the formation of gabbros. Mafic-ultramafic rocks have bulk rock and mineral compositions similar to typical Alaskan-type intrusions. The formation of these rocks probably represents the final phase of subduction-related magmatism before the juxtaposition of the accreted terrene to the Yangtze Block.

ACKNOWLEDGMENTS

This study was financially supported by the Research Grant Council of Hong Kong SAR, China (707511P), the National Natural Science Foundation of China (NSFC 41073026 and 41272212) and

a Committee on Research and Conference Grants award from Hong Kong University (201011159078). We thank L. Chen and P. Liu for EMPA analyses, J. Gao for clinopyroxene trace element analyses, G. Wang and J. Li for Re-Os analyses, and P. Xiao for Sr-Nd-Pb analyses. Thanks go to M. Grégoire for constructive comments and journal Editor D. B. Rowley for handling.

REFERENCES CITED

Ayarza, P.; Brown, D.; Alvarez-Marron, J.; and Juhlin, C. 2000. Contrasting tectonic history of the arc–continent suture in the southern and middle Urals: implications for the evolution of the orogen. J. Geol. Soc. 157:1065–1076.

Bédard, J. H. 2001. Parental magmas of the Nain Plutonic Suite anorthosites and mafic cumulates: a trace element modelling approach. Contrib Mineral. Petrol. 141:747–771.

Baier, J.; Audétat, A.; and Keppler, H. 2008. The origin of the negative niobium tantalum anomaly in subduction zone magmas. Earth Planet. Sci. Lett. 267: 290–300.

Batanova, V. G., and Sobolev, A. V. 2000. Compositional heterogeneity in subduction-related mantle peridotites, Troodos massif, Cyprus. Geology 28:55–58.

BGMRGZ (Bureau of Geology and Mineral Resources of Guizhou Province). 1987. Regional geology of Guizhou Province. Beijing, Geological (in Chinese with English abstract).

Bizimis, M.; Salters, V. J. M.; and Bonatti, E. 2000. Trace and REE content of clinopyroxenes from supra-subduction zone peridotites: implications for melting and enrichment processes in island arcs. Chem. Geol. 165: 67–85.

Brandon, A. D.; Becker, H.; Carlson, R. W.; and Shirey, S. B. 1999. Isotopic constraints on time scales and mechanisms of slab material transport in the mantle wedge: evidence from the Simcoe mantle xenoliths, Washington, USA. Chem. Geol. 160:387–407.

Brandon, A. D.; Creaser, R. A.; Shirey, S. B.; and Carlson, R. W. 1996. Osmium recycling in subduction zones. Science 272:861.

Carmichael, I. E. 1991. The redox states of basic and silicic magmas: a reflection of their source regions? Contrib. Mineral. Petrol. 106:129–141.

Chen, B.; Suzuki, K.; Tian, W.; Jahn, B.; and Ireland, T. 2009. Geochemistry and Os-Nd-Sr isotopes of the Gaositai Alaskan-type ultramafic complex from the northern North China craton: implications for mantle-crust interaction. Contrib. Mineral. Petrol. 158: 683–702.

Chen, F. K.; Li, X. H.; Wang, X. L.; Li, Q. L.; and Siebel, W. 2007. Zircon age and Nd-Hf isotopic composition of the Yunnan Tethyan belt, southwestern China. Int. J. Earth Sci. 96:1179–1194.

Chen, F. K.; Siebel, W.; Satir, M.; Terzioglu, M.; and Saka, K. 2002. Geochronology of the Karadere basement (NW Turkey) and implications for the geological evolution of the Istanbul zone. Int. J. Earth Sci. 91:469–481.

Chen, L., et al. 2011. Accurate determinations of fifty-four major and trace elements in carbonate by LA-ICP-MS using normalization strategy of bulk components as 100%. Chem. Geol. 284:283–295.

Chu, Y.; Faure, M.; Lin, W.; and Wang, Q. 2012*a*. Early Mesozoic tectonics of the South China Block: insights from the Xuefengshan intracontinental orogen. J. Asian Earth Sci. 61:199–220.

Chu, Y.; Faure, M.; Lin, W.; Wang, Q.; and Ji, W. 2012*b*. Tectonics of the Middle Triassic intracontinental Xuefengshan Belt, South China: new insights from structural and chronological constraints on the basal décollement zone. Int. J. Earth Sci. 101:2125–2150.

Conrad, W. K., and Kay, R. W. 1984. Ultramafic and mafic inclusions from Adak Island: crystallization history, and implications for the nature of primary magmas and crustal evolution in the Aleutian Arc. J. Petrol. 25:88–125.

DeBari, S. M., and Coleman, R. 1989. Examination of the deep levels of an island arc: evidence from the Tonsina ultramafic-mafic assemblage, Tonsina, Alaska. J. Geophys. Res. 94:4373–4391.

Foley, J.; Light, T.; Nelson, S.; and Harris, R. 1997. Mineral occurrences associated with mafic-ultramafic and related alkaline complexes in Alaska. Econ. Geol. 9: 396–449.

Gao, L. Z., et al. 2008. SHRIMP U-Pb zircon dating of tuff in the Shuangqiaoshan and Heshangzhen groups in South China: constraints on the evolution of the Jiangnan Neoproterozoic orogenic belt. Geol. Bull. China 27:1744–1751 (in Chinese with English abstract).

———. 2010. Zircon SHRIMP U-Pb dating of tuff bed of the Sibao Group in southeastern Guizhou: northern Guangxi area, China and its stratigraphic implication. Geol. Bull. China 29:1259–1267.

Gao, S. et al. 1999. Contrasting geochemical and Sm-Nd isotopic compositions of Archean metasediments from the Kongling high-grade terrain of the Yangtze craton: evidence for cratonic evolution and redistribution of REE during crustal anatexis. Geochim. Cosmochim. Acta 63:2071–2088.

Ge, W. C., et al. 2001. Geochemistry and geological implications of mafic-ultramafic rocks with the age of ca. 825 Ma in Yuanbaoshan-Baotan area of northern Guangxi. Geochimica 30:123–130.

Godel, B.; Barnes, S.-J.; and Maier, W. D. 2011. Parental magma composition inferred from trace element in cumulus and intercumulus silicate minerals: an example from the Lower and Lower Critical Zones of the Bushveld Complex, South Africa. Lithos 125:537–552.

Grégoire, M.; McInnes, B. I. A.; and O'Reilly, S. Y. 2001.

Hydrous metasomatism of oceanic sub-arc mantle, Lihir, Papua New Guinea. Pt. 2. Trace element characteristics of slab-derived fluids. Lithos 59:91–108.
Green, T. H. 1994. Experimental studies of trace-element partitioning applicable to igneous petrogenesis: Sedona 16 years later. Chem. Geol. 117:1–36.
Grenne, T., et al. 2003. Neoproterozoic evolution of western Ethiopia: igneous geochemistry, isotope systematics and U-Pb ages. Geol. Mag. 140:373–395.
GRGST (Guizhou Regional Geological Survey Team). 1974. Regional geological survey report of Fanjingshan area, scale 1 : 50000 (in Chinese).
Hart, S., and Kinloch, E. 1989. Osmium isotope systematics in Witwatersrand and Bushveld ore deposits. Econ. Geol. 84:1651–1655.
Hart, S. R. 1984. A large-scale isotope anomaly in the Southern Hemisphere mantle. Nature 309:753–757.
Helmy, H., and El Mahallawi, M. 2003. Gabbro Akarem mafic-ultramafic complex, Eastern Desert, Egypt: a Late Precambrian analogue of Alaskan-type complexes. Mineral. Petrol. 77:85–108.
Hermann, J.; Spandler, C.; Hack, A.; and Korsakov, A. V. 2006. Aqueous fluids and hydrous melts in high-pressure and ultra-high pressure rocks: implications for element transfer in subduction zones. Lithos 92:399–417.
Himmelberg, G. R., and Loney, R. A. 1995. Characteristics and petrogenesis of Alaskan-type ultramafic-mafic intrusions, southeastern Alaska. US Geol. Surv. Prof. Pap. 1564:1–47.
Irvine, T. 1974. Petrology of the Duke Island ultramafic complex, southeastern Alaska. Geol. Soc. Am. Mem. 138:1–244.
Jean, M. M.; Shervais, J. W.; Choi, S. H.; and Mukasa, S. B. 2010. Melt extraction and melt refertilization in mantle peridotite of the Coast Range ophiolite: an LA-ICP-MS study. Contrib. Mineral. Petrol. 159:113–136.
Johnson, K. T. M.; Dick, H. J. B.; and Shimizu, N. 1990. Melting in the oceanic upper mantle: an ion microprobe study of diopsides in abyssal peridotites. J. Geophys. Res. 95:2661–2678.
Khedr, M. Z.; Arai, S.; Tamura, A.; and Morishita, T. 2010. Clinopyroxenes in high-*P* metaperidotites from Happo-O'ne, central Japan: implications for wedge-transversal chemical change of slab-derived fluids. Lithos 119:439–456.
Kepezhinskas, P.; McDermott, F.; Defant, M. J.; Hochstaedter, A.; Drummond, M. S.; Hawkesworth, C. J.; Koloskov, A.; Maury, R. C.; and Bellon, H. 1997. Trace element and Sr-Nd-Pb isotopic constraints on a three-component model of Kamchatka Arc petrogenesis. Geochim. Cosmochim. Acta 61:577–600.
Kogiso, T.; Tatsumi, Y.; and Nakano, S. 1997. Trace element transport during dehydration processes in the subducted oceanic crust. 1. Experiments and implications for the origin of ocean island basalts. Earth Planet. Sci. Lett. 148:193–205.
Lambert, D., et al. 1994. Re-Os and Sm-Nd isotope geochemistry of the Stillwater Complex, Montana: implications for the petrogenesis of the JM Reef. J. Petrol. 35:1717–1753.
Le Bas, M. J., 1962. The role of aluminum in igneous clinopyroxenes with relation to their parentage. Am. J. Sci. 260:267–288.
Li, X. H., et al. 2003*a*. Neoproterozoic granitoids in South China: crustal melting above a mantle plume at ca. 825 Ma? Precambrian Res. 122:45–83.
———. 2009. Amalgamation between the Yangtze and Cathaysia Blocks in South China: constraints from SHRIMP U-Pb zircon ages, geochemistry and Nd-Hf isotopes of the Shuangxiwu volcanic rocks. Precambrian Res. 174:117–128.
Li, X. H.; Li, W. X.; Li, Z. X.; and Liu, Y. 2008*a*. 850–790 Ma bimodal volcanic and intrusive rocks in northern Zhejiang, South China: a major episode of continental rift magmatism during the breakup of Rodinia. Lithos 102:341–357.
Li, X. H.; Wang, X. C.; Li, W. X.; and Li, Z. X. 2008*b*. Petrogenesis and tectonic significance of Neoproterozoic basaltic rocks in South China: from orogenesis to intracontinental rifting. Geochimica 37:382–398 (in Chinese with English abstract).
Li, Z. X., et al. 2003*b*. Geochronology of Neoproterozoic syn-rift magmatism in the Yangtze Craton, South China, and correlations with other continents: evidence for a mantle superplume that broke up Rodinia. Precambrian Res. 122:85–109.
———. 2008*c*. Assembly, configuration, and break-up history of Rodinia: a synthesis. Precambrian Res. 160: 179–210.
Li, Z. X.; Li, X. H.; Kinny, P. D.; and Wang, J. 1999. The breakup of Rodinia: did it start with a mantle plume beneath South China? Earth Planet. Sci. Lett. 173:171–181.
Liu, Y., et al. 2008. In situ analysis of major and trace elements of anhydrous minerals by LA-ICP-MS without applying an internal standard. Chem. Geol. 257: 34–43.
Liu, Y. S., et al. 2010. Continental and oceanic crust recycling-induced melt-peridotite interactions in the trans-north China Orogen: U-Pb dating, Hf isotopes and trace elements in zircons from mantle xenoliths. J. Petrol. 51:537–571.
Loucks, R. R. 1990. Discrimination of ophiolitic from nonophiolitic ultramafic-mafic allochthons in orogenic belts by the Al/Ti ratio in clinopyroxene. Geology 18:346–349.
Ludwig, K. R. 2003. User's manual for Isoplot 3.00, a geochronological toolkit for Microsoft Excel. Special Publication 4. Berkeley, Berkeley Geochronological Center, p. 25–32.
Mallmann, G., and O'Neill, H. S. C. 2009. The crystal/melt partitioning of V during mantle melting as a function of oxygen fugacity compared with some other elements (Al, P, Ca, Sc, Ti, Cr, Fe, Ga, Y, Zr and Nb). J. Petrol. 50:1765–1794.
Marcantonio, F.; Reisberg, L.; Zindler, A.; Wyman, D.; and Hulbert, L. 1994. An isotopic study of the Ni-Cu-PGE-rich Wellgreen intrusion of the Wrangellia Ter-

rane: evidence for hydrothermal mobilization of rhenium and osmium. Geochim. Cosmochim. Acta 58: 1007–1018.
Maury, R. C.; Defant, M. J.; and Joron, J. L. 1992. Metasomatism of the sub-arc mantle inferred from trace elements in Philippine xenoliths. Nature 360:661–663.
McInnes, B. I. A.; Gregoire, M.; Binns, R. A.; Herzig, P. M.; and Hannington, M. D. 2001. Hydrous metasomatism of oceanic sub-arc mantle, Lihir, Papua New Guinea: petrology and geochemistry of fluid-metasomatised mantle wedge xenoliths. Earth Planet. Sci. Lett. 188:169–183.
Pettigrew, N. T.; and Hattori, K. H. 2006. The Quetico intrusions of western Superior Province: neo-Archean examples of Alaskan/Ural-type mafic-ultramafic intrusions. Precambrian Res. 149:21–42.
Qi, L.; Hu, J.; and Gregoire, D. 2000. Determination of trace elements in granites by inductively coupled plasma-mass spectrometry. Talanta 51:507–513.
Qi, L.; Zhou, M. F.; Gao, J.; and Zhao, Z. 2010. An improved Carius tube technique for determination of low concentrations of Re and Os in pyrites. J. Analyt. Atom. Spectr. 25:585–589.
Rampone, E.; Piccardo, G.; Vannucci, R.; Bottazzi, P.; and Ottolini, L. 1993. Subsolidus reactions monitored by trace element partitioning: the spinel-to plagioclase-facies transition in mantle peridotites. Contrib. Mineral. Petrol. 115:1–17.
Rivalenti, G., et al. 1996. Peridotite clinopyroxene chemistry reflects mantle processes rather than continental versus oceanic settings. Earth Planet. Sci. Lett. 139: 423–437.
Ross, K., and Elthon, D. 1993. Cumulates from strongly depleted mid-ocean-ridge basalt. Nature 365:826–829.
Rublee, V. J. 1994. Chemical petrology, mineralogy and structure of the Tulameen Complex, Princeton area, British Colombia. MSc thesis, University of Ottawa.
Rudnick, R., and Gao, S. 2003. Composition of the continental crust. *In* Treatise on geochemistry (vol. 3). Amsterdam, Elsevier, p. 1–64.
Saha, A., et al. 2005. Slab devolatilization and Os and Pb mobility in the mantle wedge of the Kamchatka arc. Earth Planet. Sci. Lett. 236:182–194.
Saleeby, J. B. 1992. Age and tectonic setting of the Duke Island ultramafic intrusion, southeast Alaska. Can. J. Earth Sci. 29:506–522.
Shirey, S. B., and Walker, R. J. 1998. The Re-Os isotope system in cosmochemistry and high-temperature geochemistry. Annu. Rev. Earth Planet. Sci. 26:423–500.
Stosch, H. G., and Seck, H. 1980. Geochemistry and mineralogy of two spinel peridotite suites from Dreiser Weiher, West Germany. Geochim. Cosmochim. Acta 44:457–470.
Suhr, G.; Seck, H.; Shimizu, N.; Günther, D.; and Jenner, G. 1998. Infiltration of refractory melts into the lowermost oceanic crust: evidence from dunite- and gabbro-hosted clinopyroxenes in the Bay of Islands Ophiolite. Contrib. Mineral. Petrol. 131:136–154.
Sun, S. S., and McDonough, W. F. 1989. Chemical and isotopic systematics of oceanic basalts: implications for mantle composition and processes. Geol. Soc. Lond. Spec. Publ. 42:313–345.
Wang, C. Y.; Zhou, M. F.; and Keays, R. R. 2006*a*. Geochemical constraints on the origin of the Permian Baimazhai mafic-ultramafic intrusion, SW China. Contrib. Mineral. Petrol. 152:309–321.
Wang, J., and Li, Z. X. 2003. History of Neoproterozoic rift basins in South China: implications for Rodinia break-up. Precambrian Res. 122:141–158.
Wang, L. J.; Griffin, W. L.; Yu, J. H.; and O'Reilly, S. Y. 2010*a*. Precambrian crustal evolution of the Yangtze Block tracked by detrital zircons from Neoproterozoic sedimentary rocks. Precambrian Res. 177:131–144.
Wang, W., et al. 2010*a*. Detrital zircon ages and Hf-Nd isotopic composition of Neoproterozoic sedimentary rocks in the Yangtze Block: constraints on the deposition age and provenance. J. Geol. 118:79–94.
Wang, W.; Chen, F. K.; Hu, R.; Chu, Y.; and Yang, Y. Z. 2012*a*. Provenance and tectonic setting of Neoproterozoic sedimentary sequences in the South China Block: evidence from detrital zircon ages and Hf-Nd isotopes. Int. J. Earth Sci. 101:1723–1744.
Wang, W., and Zhou, M.-F. 2012. Sedimentary records of the Yangtze Block (South China) and their correlation with equivalent Neoproterozoic sequences on adjacent continents. Sediment. Geol. 265–266:126–142.
Wang, W.; Zhou, M.-F.; Yan, D.-P.; and Li, J.-W. 2012*b*. Depositional age, provenance, and tectonic setting of the Neoproterozoic Sibao Group, southeastern Yangtze Block, South China. Precambrian Res. 192–195: 107–124.
Wang, W., and Zhou, M. F. 2013. Petrological and geochemical constraints on provenance, paleoweathering and tectonic setting of the Neoproterozoic sedimentary basin in the eastern Jiangnan Orogen, South China. J. Sediment. Res. 83: 974–993.
Wang, W.; Zhou, M. F.; Yan, D. P.; Li, L.; and John, M. 2013. Detrital zircon record of Neoproterozoic active-margin sedimentation in the eastern Jiangnan Orogen, South China. Precambrian Res. 235:1–19.
Wang, X. C., et al. 2008. The Bikou basalts in the northwestern Yangtze block, South China: remnants of 820–810 Ma continental flood basalts? Geol. Soc. Am. Bull. 120:1478.
Wang, X. L., et al. 2006*b*. LA-ICP-MS U-Pb zircon geochronology of the Neoproterozoic igneous rocks from northern Guangxi, South China: implications for tectonic evolution. Precambrian Res. 145:111–130.
Weaver, B. L., 1991. The origin of ocean island basalt end-member compositions: trace element and isotopic constraints. Earth Planet Sci Lett. 104:381–397.
Widom, E.; Kepezhinskas, P.; and Defant, M. 2003. The nature of metasomatism in the sub-arc mantle wedge: evidence from Re–Os isotopes in Kamchatka peridotite xenoliths. Chem. Geol. 196:283–306.
Wilson, M. 1989. Igneous petrogenesis. London, Unwin Hyman, p. 245–285.
Wu, R. X., et al. 2006. Reworking of juvenile crust: element and isotope evidence from Neoproterozoic

granodiorite in South China. Precambrian Res. 146: 179–212.

Xiong, X., Adam, J., and Green, T. 2005. Rutile stability and rutile/melt HFSE partitioning during partial melting of hydrous basalt: implications for TTG genesis. Chem. Geol. 218:339–359.

Xue, H. M.; Ma, F.; and Song, Y. Q. 2012. Mafic-ultramafic rocks from the Fanjingshan region, southwestern margin of the Jiangnan orogenic belt: ages, geochemical characteristics and tectonic setting. Acta Petrol. Sin. 28:3015–3030.

Yan, D. P.; Zhou, M. F.; Song, H. L.; Wang, X. W.; and Malpas, J. 2003. Origin and tectonic significance of a Mesozoic multi-layer over-thrust system within the Yangtze Block (South China). Tectonophysics 361: 239–254.

Yang, S. H., et al. 2012. Selective crustal contamination and decoupling of lithophile and chalcophile element isotopes in sulfide-bearing mafic intrusions: an example from the Jingbulake Intrusion, Xinjiang, NW China. Chem. Geol. 302–303:106–118.

Zhang, H.; Wang, M.; and Zheng, Q.-Q. 2008. The character and its significance of magnesio-ferri-ultramagnesio-ferri irruptive rock in Fanjingshan Mountain area. Guizhou Geol. 25:161–165 (in Chinese with English abstract).

Zhang, J. L. 2008. The Sr-Nd-Pb isotopic geochemistry of Kongling high grade terrain of the Yangtze Craton (South China) and its tectonic implications. MPhil thesis, Wuhan, University of Geosciences.

Zhang, S. B.; Wu, R. X.; and Zheng, Y. F. 2012*a*. Neoproterozoic continental accretion in South China: geochemical evidence from the Fuchuan ophiolite in the Jiangnan orogen. Precambrian Res. 220–221:45–64.

Zhang, Y. Z.; Wang, Y. J.; Fan, W. M.; Zhang, A. M.; and Ma, L. Y. 2012*b*. Geochronological and geochemical constraints on the metasomatised source for the Neoproterozoic (~825 Ma) high-Mg volcanic rocks from the Cangshuipu area (Hunan Province) along the Jiangnan Domain and their tectonic implications. Precambrian Res. 220–221:139–157.

Zhao, G., and Cawood, P. A. 2012. Precambrian geology of China. Precambrian Res. 222–223:13–54.

Zhao, J.-H., and Zhou, M.-F. 2013. Neoproterozoic high-Mg basalts formed by melting of ambient mantle in South China. Precambrian Res. 233:193–205.

———. 2007. Geochemistry of Neoproterozoic mafic intrusions in the Panzhihua district (Sichuan Province, SW China): implications for subduction-related metasomatism in the upper mantle. Precambrian Res. 152: 27–47.

Zhao, J. H.; Zhou, M. F.; Yan, D. P.; Zheng, J. P.; and Li, J. W. 2011. Reappraisal of the ages of Neoproterozoic strata in South China: no connection with the Grenvillian orogeny. Geology 39:299–302.

Zheng, L.; Zhi, X.; and Reisberg, L. 2009. Re-Os systematics of the Raobazhai peridotite massifs from the Dabie orogenic zone, eastern China. Chem. Geol. 268: 1–14.

Zheng, Y.-F.; Xiao, W.-J.; and Zhao, G. 2013. Introduction to tectonics of China. Gondwana Res. 23:1189–1206.

Zheng, Y. F., et al. 2008. Rift melting of juvenile arc-derived crust: geochemical evidence from Neoproterozoic volcanic and granitic rocks in the Jiangnan Orogen, South China. Precambrian Res. 163:351–383.

Zhou, J. C.; Wang, X. L.; and Qiu, J. S. 2008. Is the Jiangnan orogenic belt a Grenvillian orogenic belt: some problems about the Precambrian geology of South China. Geol. J. China Univ. 14:64–72 (in Chinese with English abstract).

Zhou, J. C.; Wang, X. L.; and Qiu, J. S. 2009. Geochronology of Neoproterozoic mafic rocks and sandstones from northeastern Guizhou, South China: coeval arc magmatism and sedimentation. Precambrian Res. 170:27–42.

Zhou, M. F.; Yan, D. P.; Kennedy, A. K.; Li, Y. Q.; and Ding, J. 2002. SHRIMP zircon geochronological and geochemical evidence for Neoproterozoic arc-related magmatism along the western margin of the Yangtze Block, South China. Earth Planet. Sci. Lett. 196:51–67.

Zindler, A., and Hart, S. 1986. Chemical geodynamics. Ann. Rev. Earth Planet. Sci. 14:493–571.